JOURNAL OF MATERIALS SCIENCE 22 (1987) 2319–2326

# Accelerated spheroidization of cementite in high-carbon steel wires by drawing at elevated temperatures

SEUNG EUI NAM
*Department of Metallurgical Engineering, Hong Ik University, Sogyo-dong, Sodaemun-gu, Seoul, Korea*

DONG NYUNG LEE
*Department of Metallurgical Engineering, Seoul National University, Shillim-dong, Kwanak-gu, Seoul, Korea*

The spheroidization of cementite lamellae in high-carbon steel wires could be achieved in a short time by drawing at elevated temperatures below the $A_1$ temperature. The rapid spheroidization was attributed mainly to shearing or fracturing of cementite plates into smaller particles. Sharp edges of the fractured particles were thought to be blunted by the diffusion of iron and carbon atoms. The diffusion rate in the case of drawing at elevated temperatures was very rapid compared with that in the case of static annealing, due to continuous regeneration of dislocations and vacancies during the drawing. However, the mechanical properties of the spheroidized wires were deteriorated by internal voids formed during the drawing. Such a disadvantage could be circumvented by many cold-drawing passes followed by a final single drawing pass at an elevated temperature.

## 1. Introduction

The formability and machinability of steels can be enhanced by spheroidizing the cementite lamellae in pearlite. The spheroidization of cementite can be achieved by annealing slightly below the $A_1$ temperature [1, 2]. The process can be enhanced by cyclic heating near the $A_1$ temperature [3, 4], by cold-working prior to annealing [2], and further by plastic deformation at elevated temperatures below the $A_1$ temperature [5–12]. The plastic deformation at elevated temperatures has been made mostly by rolling or torsion. Another method of spheroidization is quenching, followed by tempering for a long time, but the method is hardly applied to high-carbon steel wires.

The purpose of this work is to accelerate the spheroidization of cementite lamellae in high-carbon steels by rod or wire drawing at temperatures slightly below the $A_1$ temperature.

## 2. Experimental methods

Commercially available high-carbon steel wire rods of 5.5 to 13 mm diameter were used and their chemical composition is given in Table I.

The high-carbon steel wire rods were mechanically descaled with emery paper and coated with a wet

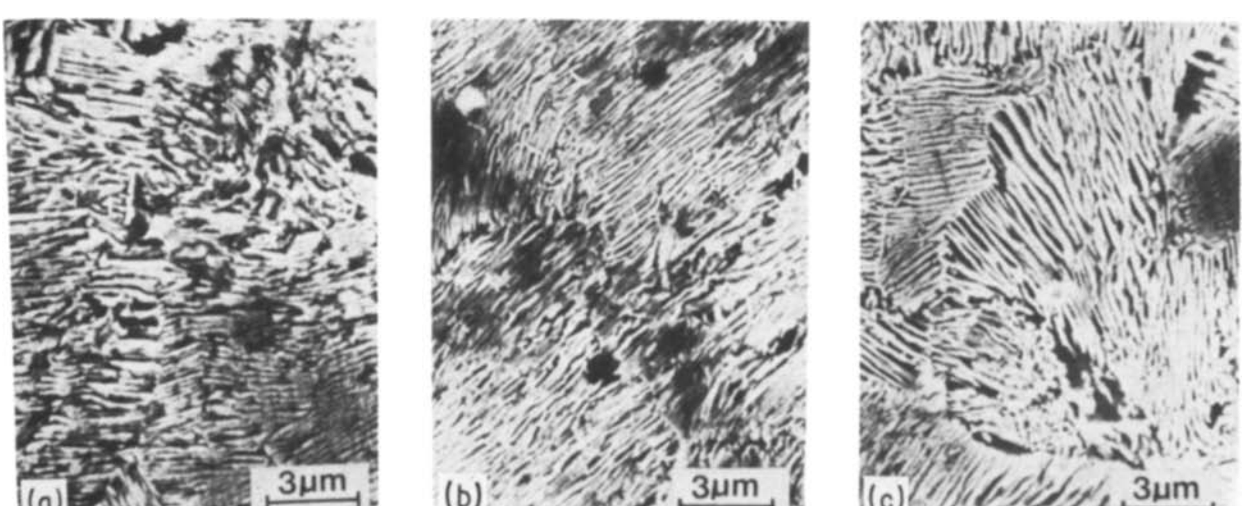


*Figure 1* Scanning electron micrographs showing pearlite structures of the specimens: (a) WR-1, (b) WR-3, (c) WR-5.

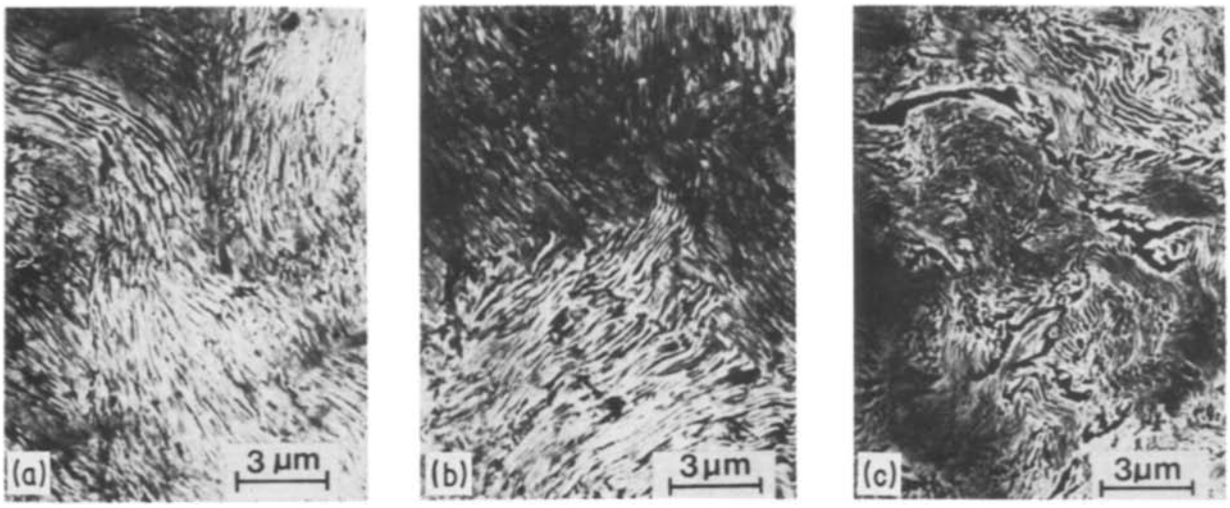


*Figure 2* Scanning electron micrographs of pearlite structures in the specimens deformed by cold drawing: (a) WR-1 specimen reduced by 62%, (b) WR-3 specimen reduced by 64%, (c) WR-5 specimen reduced by 67%.

lubricant composed of $MoS_2$ and graphite powders, followed by drying. The wire rods were subsequently heated at predetermined temperatures in an electric tube furnace for about 5 min and then drawn at a speed of $10\,\mathrm{m\,min^{-1}}$ on a draw bench. Some wires were drawn at room temperature and then annealed.

Microstructures of the cross-sections of specimens were examined on transmission and scanning electron microscopes. The Vickers hardness of the cross-sections was measured at a load of 500 g. Tensile testing of the wire specimens was conducted on an Instron machine at a crosshead speed of $1\,\mathrm{cm\,min^{-1}}$. The tensile specimens were fabricated in accordance with ASTM standards E8-69. The gauge length of tensile specimens of 6 mm or more in diameter was four times the diameter, and was 10 cm for specimens of diameter less than 6 mm. The density of a wire sample was evaluated by measuring its weight, length and diameter.

## 3. Results and discussion

The interlamellar spacings of pearlite in the wire rods were mostly in the range of 0.12 to 0.15 $\mu$m as shown in Fig. 1. When the rods were drawn at room temperature, a wavy pearlite structure was developed as shown in Fig. 2, which implies that deformation of the pearlite was mostly plastic even though fracture of it in part could not be excluded. This is in agreement with Langford's compilation (Fig. 3). However, the spheroidization and growth of cementite particles were substantially enhanced by drawing at elevated temperatures slightly below the $A_1$ point. Fig. 4 shows an example of sequential changes in microstructures of wires drawn at elevated temperatures. The wires were heated at 700° C for 5 min prior to each drawing pass. Even a single pass of drawing at 700° C achieved a substantial spheroidization of cementite, and further spheroidization and growth of cementite particles were achieved by the repeated drawings.

Transmission electron micrographs of various parts of WR-1 wire drawn by 15% at 700° C show almost intact cementite lamellae, severely bent cementite lamellae, some of which were sheared or fractured, and sheared cementite particles (Fig. 5). Such differences in the microstructure of cementite were thought to be caused by differences in the angle between the cementite lamella orientation and the wire axis. For example, the cementite lamellae oriented parallel to the wire axis would be more difficult to fracture than any other cementite lamellae with different orientations. The microstructures in Fig. 5 suggest that the accelerated spheroidization of cementite by drawing at elevated temperatures could be attributed to shearing or fracturing of cementite plates into smaller particles during the drawing. Sharp edges of the sheared or fractured particles could be blunted by the diffusion of carbon and iron atoms during the drawing, and

TABLE I Chemical composition of materials

| Wire | Composition (wt %) C | Si | Mn | P | S | Cu |
|---|---|---|---|---|---|---|
| WR-1 | 0.85 | 0.25 | 0.74 | 0.022 | 0.019 | – |
| WR-2 | 0.79 | 0.20 | 0.75 | 0.020 | 0.016 | – |
| WR-3 | 0.74 | 0.28 | 0.72 | 0.020 | 0.018 | – |
| WR-4 | 0.68 | 0.21 | 0.77 | 0.019 | 0.006 | – |
| WR-5 | 0.65 | 0.21 | 0.66 | 0.017 | 0.015 | 0.2 |

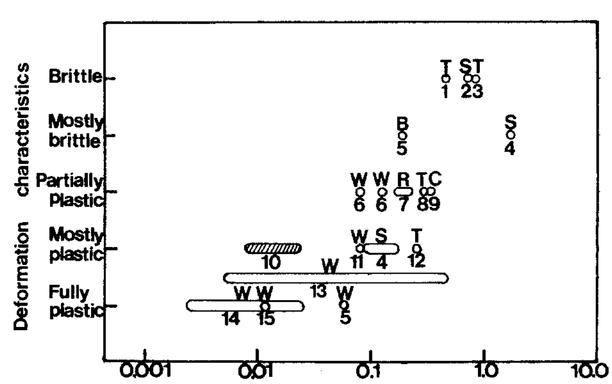


*Figure 3* A size effect in the plastic deformability of the cementite lamellae in pearlite [12]. (O, ⬭) Indirect evidence, (⬭) direct observations; B = bending of wires, C = compression, R = rolling of sheet, S = swaging of wires, T = tension, W = wire drawing.

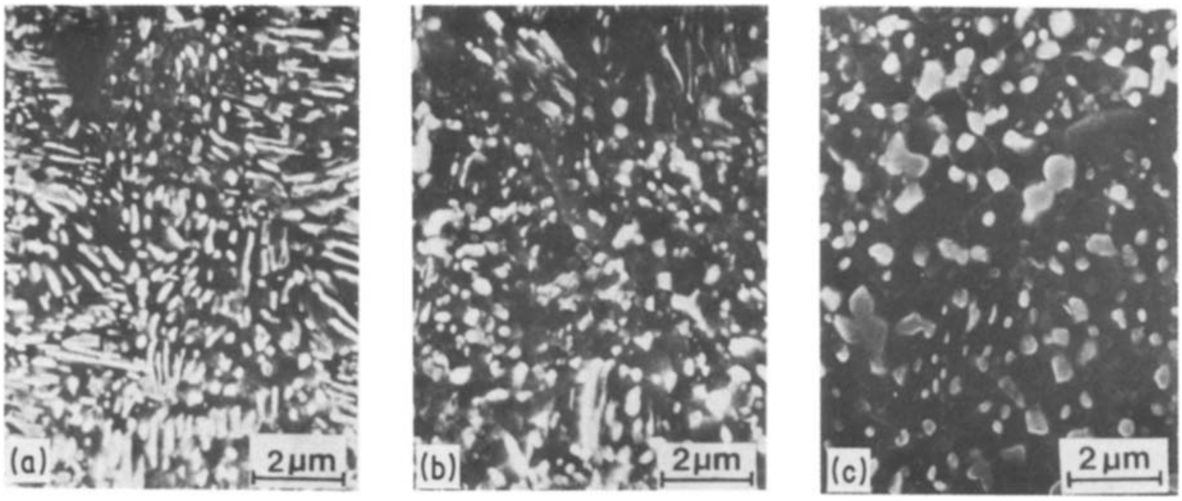


*Figure 4* Scanning electron micrographs of WR-3 specimens drawn by (a) 21% (1 pass), (b) 44.3% (3 passes) and (c) 60% (5 passes) at 700° C.

much more during subsequent heating. An extremely high diffusion rate can be obtained during deformation at high temperatures; because dislocations and vacancies are continually generated.

For a quantitative assessment of the spheroidization it is necessary to define shape factors or aspect ratios of the spheroidized particles. Fig. 6 shows the shape distributions of cementite particles in WR-1, 3 and 5 wires drawn by one pass (21% reduction) at 700° C. The maximum frequency occurred at an aspect ratio of about two, and the population of particles having an aspect ratio of less than three was over 80% in the specimens. The particles whose aspect ratios were less than three were assumed to be spheroidized in this paper.

The volume fraction of spheroidized cementite particles increased with increasing carbon content, drawing reduction and temperature as shown in Fig. 7. The increase in reduction ratio is expected to cause fracture of an increasing number of cementite particles, which in turn increases the spheroidization of cementite particles. The increase in carbon content

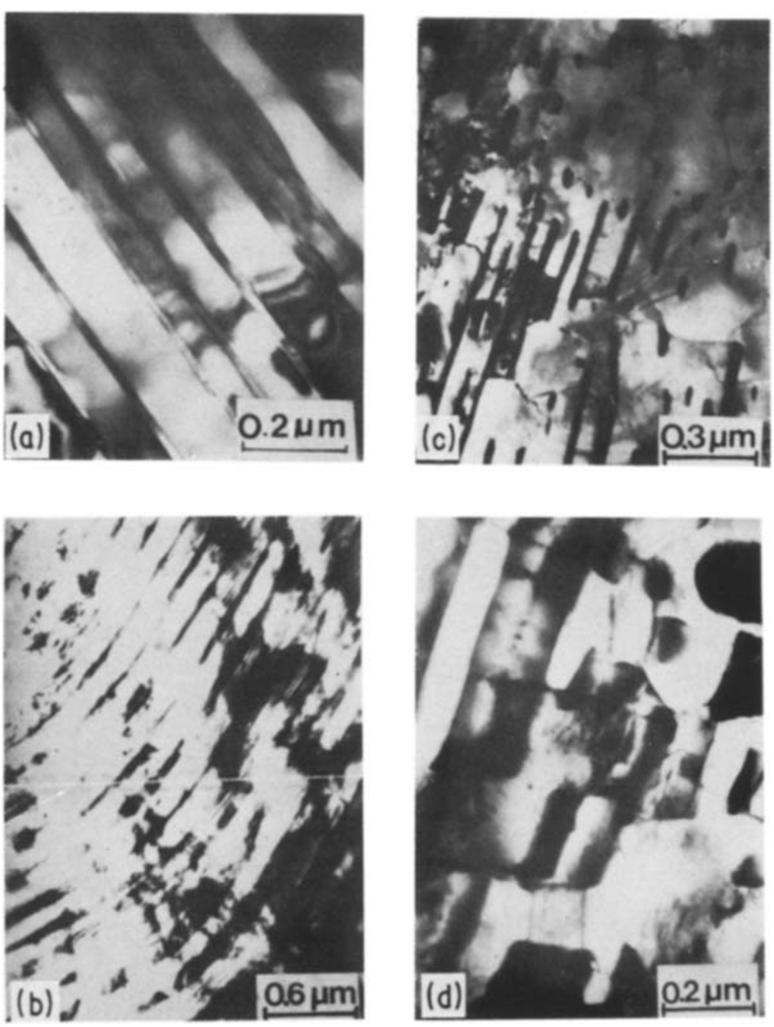


*Figure 5* Transmission electron micrographs of various areas of 0.85% C steel wire drawn by 15% at 700° C. (a) Area of cementite lamellae; (b) severely bent cementite lamellae, some of which are sheared or fractured; (c) and (d) areas showing sheared cementite particles.

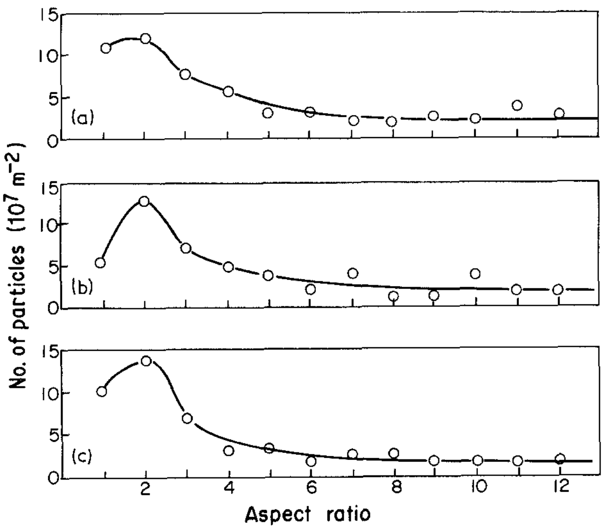


*Figure 6* Aspect ratio against number of cementite particles in steel wires drawn by 21% at 700° C; (a) WR-1, (b) WR-3, (c) WR-5.

means an increase in the ratio of the amounts of cementite and ferrite. When a two-phase alloy composed of soft and hard phases is subjected to plastic deformation, the deformation is larger in the soft phase than in the hard phase. However, as the volume percentage of the hard phase increases, the strains in the two phases approach the same value. Therefore the increase in carbon content (i.e. the increase in cementite content) increases the deformation of pearlite, which in turn increases the spheroidization of cementite particles. The increase in the volume fraction of spheroidized cementite particles with increasing drawing temperature as shown in Fig. 7, and the plastic deformability of the cementite lamellae in pearlite in cold-drawn wires as shown in Fig. 3, indicate that the plastic deformability of the cementite lamellae decreases with increasing drawing temperature.

The results in Fig. 7 indicate that the spheroidiza-

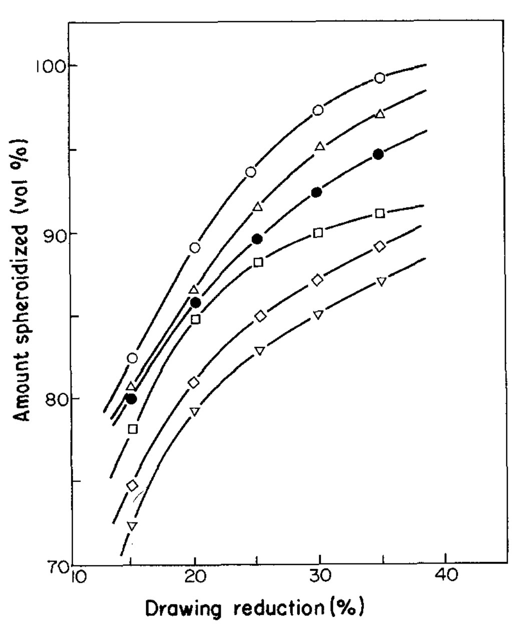


*Figure 7* Volume percentage of spheroidized cementite particles as a function of drawing reduction: (○) WR-1, 700° C; (△) WR-3, 700° C; (●) WR-5, 700° C; (□) WR-1, 650° C; (◇) WR-2, 650° C; (▽) WR-3, 650° C.

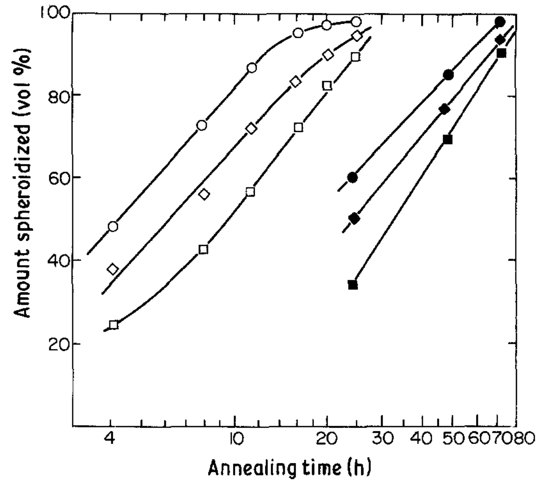


*Figure 8* The spheroidization rate of cementite in WR-1, 2 and 4 wires, when annealed at 700° C without prior cold drawing, and after cold drawing by 62% (WR-1), 78% (WR-2) and 77% (WR-4). D = cold-drawn samples, N = normalized samples: (○) WR-1,D; (◇) WR-2,D; (□) WR-4,D; (●) WR-1,N; (◆) WR-2,N; (■) WR-4,N.

tion of cementite could be achieved during drawing of the steel wires, if the cementite particle size is not taken into consideration. This is an extremely rapid spheroidization of cementite compared with those by conventional methods as shown in Fig. 8. Fig. 8 shows the spheroidization rates of cementite in the wires of WR-1, 2 and 4, when annealed at 700° C without prior cold-drawing and after cold-drawing. For example, the wire of WR-2,D, which was annealed at 700° C for 24 h after cold-drawing by 78%, achieved 95% spheroidization, whereas the wire of WR-2,N, which was annealed at 700° C for 24 h without prior cold-drawing, achieved only 45% spheroidization. The enhanced spheroidization of cementite in the cold-drawn wires may be attributed to possible fracture of cementite particles during drawing, which was not resolved in the microstructures, and to the vacancy concentration and dislocation density being increased during drawing. The increase in spheroidization with increasing carbon concentration in Fig. 8 may be attributed not only to increased fracture of cementite particles in cold-drawn wires as pointed out in the explanation of the results in Fig. 7, but also to a decreased diffusion distance due to decreased interlamellar spacing; otherwise the difference in the volume percentage spheroidized among WR-1,N, WR-2,N, and WR-4,N could not be expected since they were not subjected to plastic deformation before annealing. Fig. 9 shows the spheroidized cementite particles in WR-1 wire specimens prepared by annealing at 700° C without prior cold-drawing and after cold-drawing.

The drawing at 700° C could also cause a rapid growth of cementite particles. Fig. 10 shows the cube of the mean cementite particle radius as a function of total heating time at intervals of drawing of WR-3 wire at 700° C. Initial cementite particles were spheroidized by a drawing reduction by 21% at 700° C. This figure implies a diffusion-controlled growth of cementite particles, which may be expressed by the

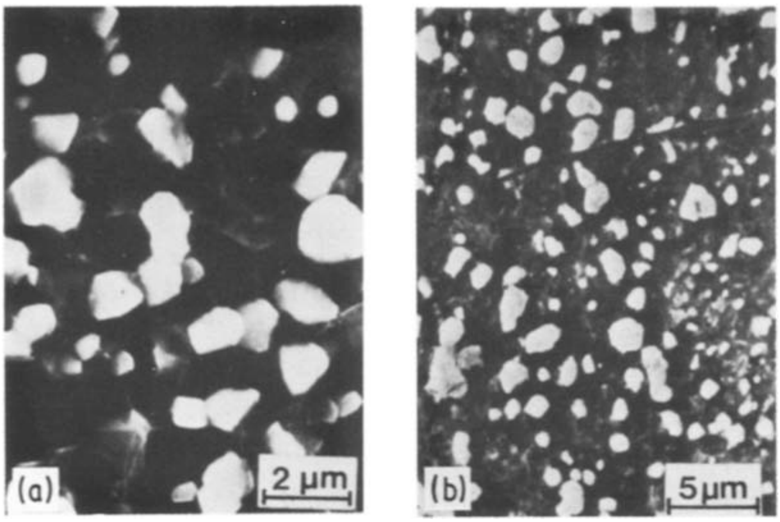


*Figure 9* The spheroidized cementite particles in WR-1 wires annealed at 700° C for 72 h (a) without prior cold drawing and (b) annealed at 700° C for 24 h after cold drawing by 62%.

following relation [8]:

$$r^3 - r_0^3 = \alpha\gamma V_{Fe_3C} X_c \bar{D}_c t / V_{Fe} RT \quad (1)$$

where $r$ and $r_0$ are mean particle radii at times $t$ and $t_0$, $\gamma$ is the interface energy, $X_c$ is the mole fraction of carbon in equilibrium between ferrite and cementite, $\bar{D}_c$ is the effective diffusion coefficient of carbon, $\alpha$ is a constant ($= 8/9$) [8] and $t$ is time. Substitution of appropriate quantities, $\gamma = 5 \times 10^{-7}\,\mathrm{J\,mm^{-2}}$, $V_{Fe_3C} = 23.97 \times 10^3\,\mathrm{mm^3\,mol^{-1}}$, $V_{Fe} = 7.3 \times 10^3\,\mathrm{mm^3\,mol^{-1}}$, $X_c = 7.7 \times 10^{-4}$, $R = 8.32\,\mathrm{J\,K^{-1}\,mol^{-1}}$ and $T = 973\,\mathrm{K}$, into Equation 1 and the measured slope of Fig. 10 yields $\bar{D}_c = 2.55 \times 10^{-6}\,\mathrm{mm\,sec^{-1}}$, which is one order of magnitude larger than $\bar{D}_c = 3.16 \times 10^{-7}\,\mathrm{mm\,sec^{-1}}$ obtained by static annealing at 700° C (see Fig. 11). This enhanced value of diffusion coefficient is thought to be associated with vacancies and dislocations generated continually during the deformation at elevated temperature. The aspect ratios of the spheroidites might be argued to influence the diffusion process. Since the aspect ratios of the spheroidites approached one after two drawing passes, $\bar{D}_c$ obtained from Fig. 10 seems to be little affected by the aspect ratio.

The wire drawing at an elevated temperature had, however, disadvantages including not only general inconvenience in the hot-working, but also internal voids formed in the wire by the repeated drawings, which was manifested by the density of the wire. The density decreased with increasing drawing reduction as shown in Fig. 12 due to internal void formation (drawing true strain = ln[1/(1 − drawing reduction)]). The elongation of wires increased and then decreased with increasing drawing reduction as shown in Fig. 13, while the tensile strength decreased with increasing drawing reduction as shown in Fig. 14. The mechanical behaviour can be explained by the spheroidization and particle growth of cementite and by internal void formation. The spheroidization and

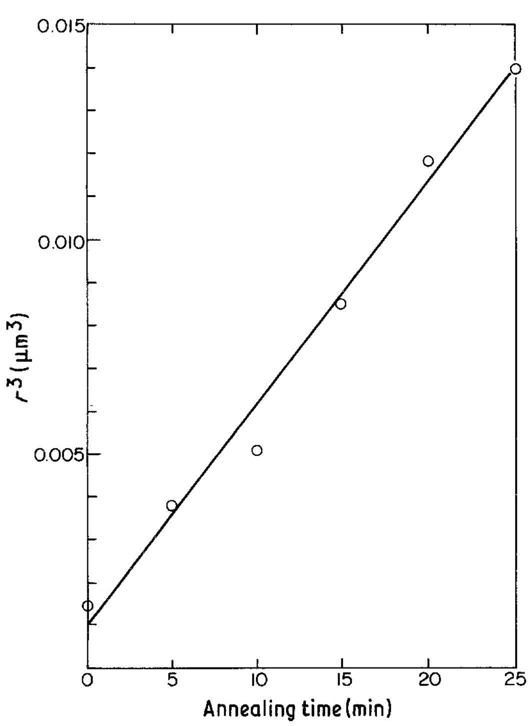


*Figure 10* Cube of mean cementite particle radius as a function of total heating time at intervals of drawing of WR-3 wire at 700° C. Initial cementite particles were spheroidized by drawing by 21% at 700° C. Reduction per drawing pass ranged between 15 and 20%. Slope = $5.15 \times 10^{-4}\,\mu m^3\,min^{-1}$.

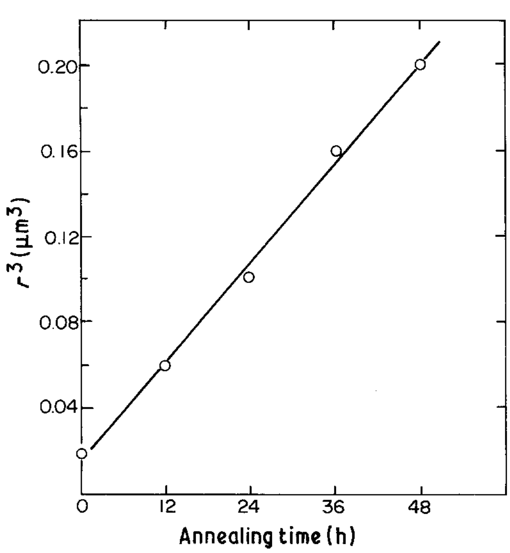


*Figure 11* Cube of mean cementite particle radius in WR-1 wire as a function of annealing time at 700° C. Initial cementite particles were already spheroidized by annealing at 700° C for 24 h after cold drawing by 62%. Slope = $6.39 \times 10^{-5}\,\mu m^3\,min^{-1}$.

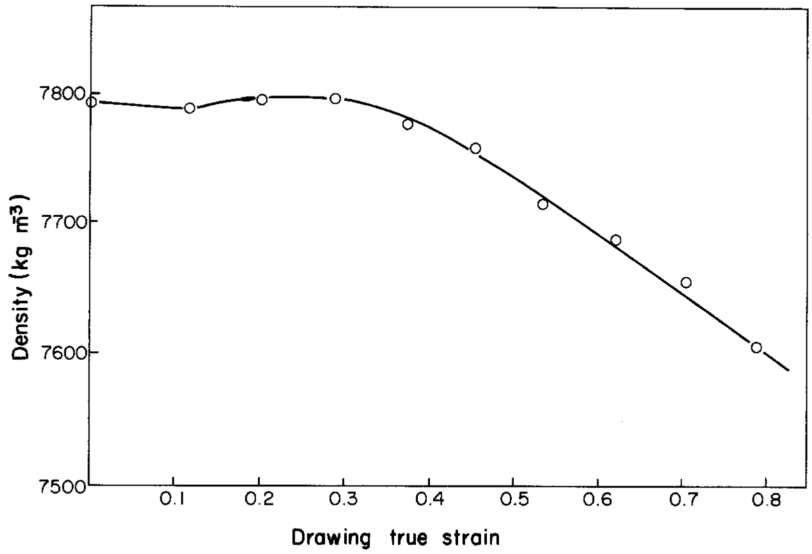


*Figure 12* The density of WR-5 wire as a function of drawing true strain. Drawing true strain is defined as the natural logarithm of the ratio of cross-sectional areas before and after deformation.

growth of cementite particles would decrease the tensile strength (Fig. 15) and the hardness (Fig. 16) and increase the elongation (Fig. 15), whereas the void formation would decrease both the tensile strength and the yield strength. The data in Fig. 15 were obtained from WR-1, 2 and 4 wires which were annealed at 700° C without prior deformation and had few internal defects. Therefore the effects of internal voids were thought to be excluded in Fig. 15.

The disadvantages caused by the repeated drawings at elevated temperatures could be circumvented by many cold-drawing passes (much cold reduction), followed by the final single drawing pass at an elevated temperature. Fig. 17 shows an example of such cases, where WR-1 wire was reduced by 65% at room temperature and then drawn by 13% at 700° C, and 100% spheroidization was achieved.

Unlike normalized high-carbon steel wires, the stress–strain curves of the spheroidized steel wires showed the yield point phenomenon and the Portevin LeChatelier effect, which are often observed in low-carbon steels as shown in Fig. 18. The behaviour reflects the important role that ferrite plays in the deformation, since the spheroidized cementites are embedded in the softer ferrite phase.

## 4. Conclusions

1. The spheroidization of cementite lamellae in

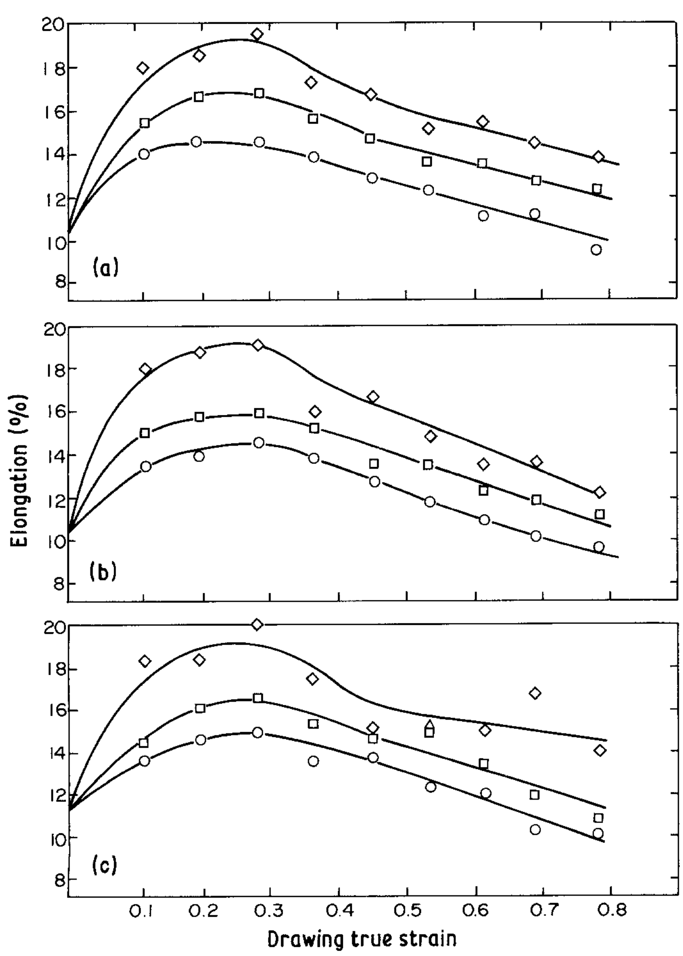


*Figure 13* The elongations of (a) WR-1, (b) WR-3 and (c) WR-5 wires as a function of drawing true strain; (○) 600° C, (□) 650° C, (◇) 700° C.

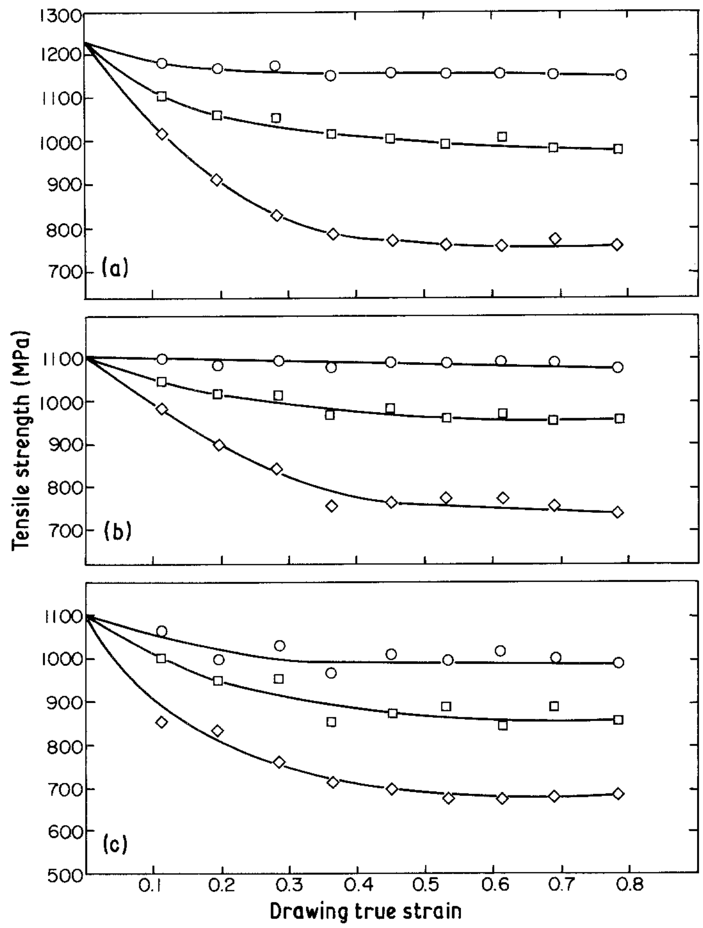


*Figure 14* The tensile strengths of (a) WR-1, (b) WR-3 and (c) WR-5 wires as a function of drawing true strain at 700° C: (○) 600° C, (□) 650° C, (◇) 700° C.

high-carbon steel wires could be achieved by a few successive drawings at 700° C.

2. The volume fraction of spheroidized cementite particles increased with increasing carbon content, drawing reduction and temperature.

3. A principal mechanism of the spheroidization appeared to be shearing or fracturing of cementite lamellae into smaller particles whose sharp edges became subsequently blunted by the diffusion of iron and carbon atoms.

4. The diffusion was thought to be extremely enhanced by the regeneration of dislocations and vacancies during the high-temperature deformation.

5. The enhanced diffusion was manifested by the higher growth rate of cementite particles in the specimens deformed at high temperatures compared with the specimens annealed statically.

6. As the spheroidization by drawing at elevated temperatures progressed, the tensile strength of the wires decreased, while the elongation increased and then decreased.

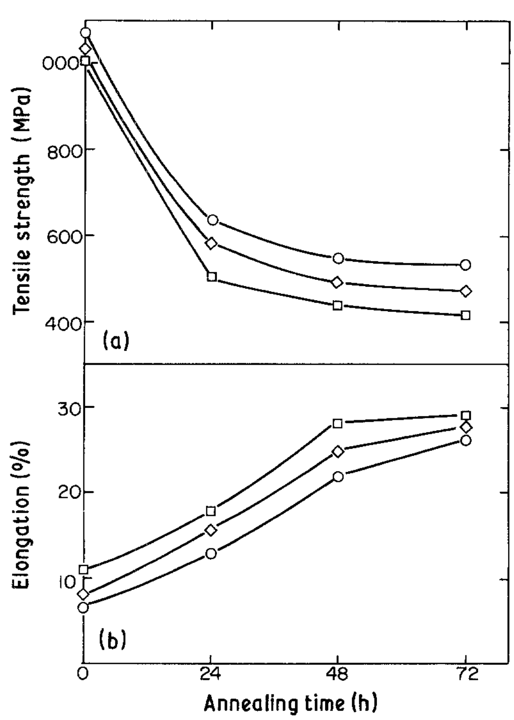


*Figure 15* (a) Tensile strengths and (b) elongations of (○) WR-1, (◇) WR-2 and (□) WR-4 wires as a function of annealing time at 700° C.

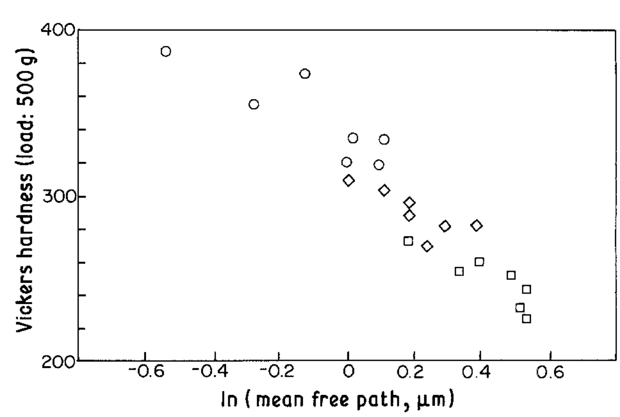


*Figure 16* The hardness of wires drawn at various temperatures as a function of linear mean free path: (○) 600° C, (◇) 650° C, (□) 700° C.

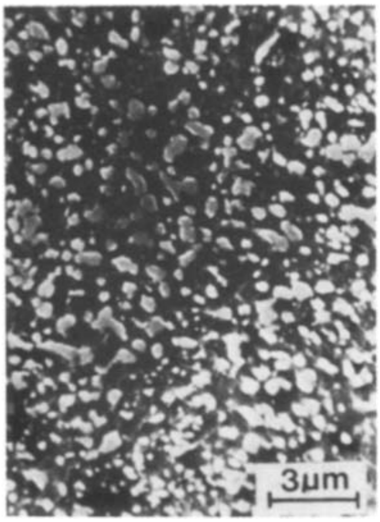


*Figure 17* The microstructure of WR-1 wire cold drawn by 65%, followed by 13% drawing at 700° C.

7. The decrease in the elongation was attributed to the internal voids formed by the high-temperature drawing.

8. Internal void formation could be circumvented by sufficient passes of cold drawing followed by one final drawing pass at an elevated temperature.

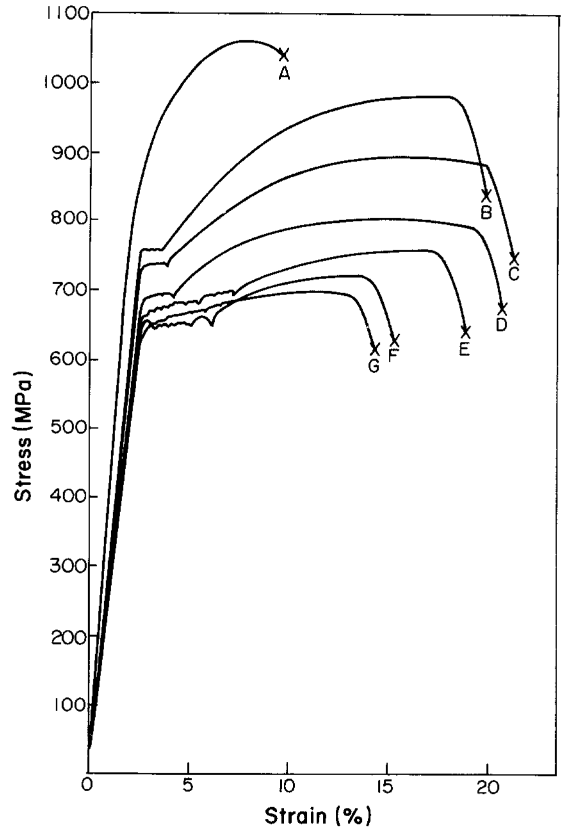


*Figure 18* The stress–strain curves of WR-3 wires drawn at 700° C. Specimen diameters and area reductions as follows: (A) 5.50 mm, 0%; (B) 4.90 mm, 21%; (C) 4.50 mm, 33%; (D) 4.13 mm, 44%; (E) 3.80 mm, 52%; (F) 3.50 mm, 60%; (G) 3.22 mm, 66%. Crosshead speed: 10 mm min$^{-1}$.

## References


1. C. M. SELLAR, *Metallography* **10** (1977) 89.
2. A. H. HOLTZMAN, J. C. DANKO and R. D. STOUT, *Trans. Met. Soc. AIME* **212** (1958) 475.
3. J. LEEDER, P. PAYSON and W. L. HODAPP, *Trans. ASM* **28** (1940) 306.
4. O. E. CULLEN, *Met. Progr.* **64** (1953) 78.
5. J. L. ROBBINS, O. C. SHEPARD and O. D. SHERBY, *J. Iron Steel Inst.* **202** (1964) 804.
6. O. D. SHERBY, M. J. HARRIGAN, L. SHAMAG and C. SAUVE, *Trans. ASM* **21** (1969) 578.
7. E. A. CHOJNOWSKI and W. J. McG. TEGART, *Met. Sci. J.* **2** (1968) 14.
8. A. G. MARTIN and C. M. SELLAR, *Metallography* **3** (1970) 259.
9. D. F. LUPTON and D. H. WARRINGTON, *Met. Sci. J.* **6** (1972) 200.
10. S. CHATTOPADHYAY and C. M. SELLARS, *Acta Metall.* **30** (1982) 157.
11. S. E. NAM and D. N. LEE, *J. Korean Inst. Met.* **19** (1981) 143.
12. *Idem*, in "Strength of Metals and Alloys", edited by H. J. McQueen, J.-P. Bailon, J. I. Dickson, J. J. Jonas and M. G. Akben (Pergamon, Oxford, 1985) p. 1061.



*Received 28 January and accepted 30 June 1986*